

# Simulation and Investigation of Random Grain-Boundary-Induced Variabilities for Stackable NAND Flash Using 3-D Voronoi Grain Patterns

Ching-Wei Yang and Pin Su, *Member, IEEE*

**Abstract**—This brief investigates the random grain-boundary (GB)-induced variability in poly-crystalline silicon thin-film transistor for stackable NAND flash applications using 3-D Voronoi grain patterns. Compared with the 1-D and 2-D methods, the 3-D Voronoi grain can show a more realistic threshold-voltage variability when devices are downscaled along the channel height ( $H_{ch}$ ) direction. Therefore, a full 3-D consideration is needed when modeling the random GB-induced variation.

**Index Terms**—3-D NAND, grain boundary (GB), variability, Voronoi.

## I. INTRODUCTION

TO ACHIEVE higher data storage density, NAND flash memories have been aggressively scaled down. Building 3-D array for NAND flash memories with multilayers and few critical process steps is one way to pursue higher bit density and lower bit cost simultaneously [1]. Various 3-D NAND flash array structures have been proposed recently [2]–[6]. However, these 3-D structures may suffer significant variability because most of them adopt poly-crystalline silicon (poly-Si) channel, which possesses random traps [7]. It has been reported that the random trap fluctuation has a noticeable influence on the threshold-voltage ( $V_T$ ) distribution [8]. Therefore, an adequate modeling of the trap states in poly-Si is crucial to analyzing the device characteristics. To investigate the  $V_T$  fluctuations, poly-Si channel was modeled as Si material with traps introduced uniformly throughout the channel in the past [9]. This modeling method may be accurate for large devices possessing many grains in the active region. However, as the device size downscales, this model fails to capture the fact that the trap states are concentrated at the Si grain boundaries (GBs). In other words, more attention on the actual locations of GBs where the device variability stems from is needed.

There are several works [7], [10]–[13], [20]–[22] engaging in modeling and simulating the effects of randomly located GBs in poly-Si channel. In [11], devices with equally

Manuscript received October 31, 2013; accepted February 18, 2014. Date of current version March 20, 2014. This work was supported in part by the National Science Council of Taiwan under Contract NSC 102-2221-E-009-136-MY2 and in part by the Ministry of Education in Taiwan through the ATU Program. The review of this brief was arranged by Editor H. S. Momose.

The authors are with the Department of Electronics Engineering, Institute of Electronics, National Chiao Tung University, Hsinchu 30010, Taiwan (e-mail: oranfrog.eecs96@g2.nctu.edu.tw; pinsu@faculty.nctu.edu.tw).

Color versions of one or more of the figures in this paper are available online at <http://ieeexplore.ieee.org>.

Digital Object Identifier 10.1109/TED.2014.2308951

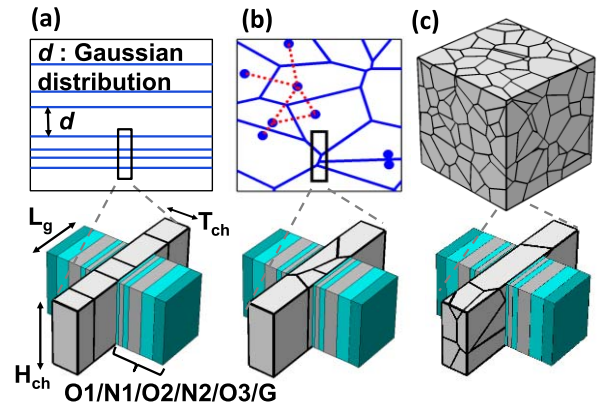


Fig. 1. Schematics for (a) 1-D rectangular [12], (b) 2-D Voronoi [13], and (c) 3-D Voronoi GBs.

spaced GBs (namely, the grain size and the shape of grains are fixed) were simulated and analyzed. In [12], a 1-D rectangular method was used to consider the Si grain size variation by assuming a Gaussian distributed grain size with a given mean value and standard deviation. In the above two methods, the GBs have always been assumed to be perpendicular to the path where carriers flow. In other words, the shape of grain is constrained as rectangles and the GB is 1-D. This assumption, however, ignores the nature of arbitrary shape of grain patterns, and is unrealistic.

In this brief, utilizing a novel 3-D Voronoi method, we investigate the GB-induced variability for 3-D NAND flash. This brief is organized as follows. In Section II, we describe our methodology to simulate random GB-induced variation. The  $V_T$  variation caused by random GBs is investigated in Section III. The conclusion is drawn in Section IV.

## II. SIMULATION METHODOLOGY

Fig. 1 shows a summary of schematics and simulation methodologies employed in this brief. 1-D rectangular [12], 2-D Voronoi [13], [14], and 3-D Voronoi GB patterns are all performed for comparison. To reach a fair comparison, we perform 3-D simulations for both 1-D and 2-D grain patterns by extending the channel region along the width direction and redefine it as channel height ( $H_{ch}$ ).

The flow chart for both 2-D and 3-D Voronoi approaches to simulate random GB-induced variation is shown in Fig. 2. The input parameter is the average grain size ( $d$ ). For a given grain

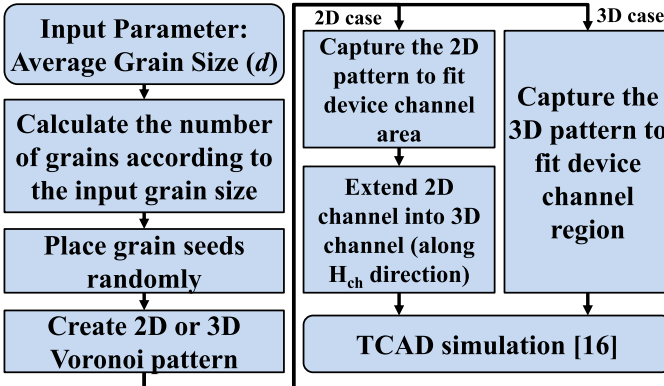


Fig. 2. Flow chart describing the 2-D and 3-D Voronoi methods for simulating poly-Si channels.

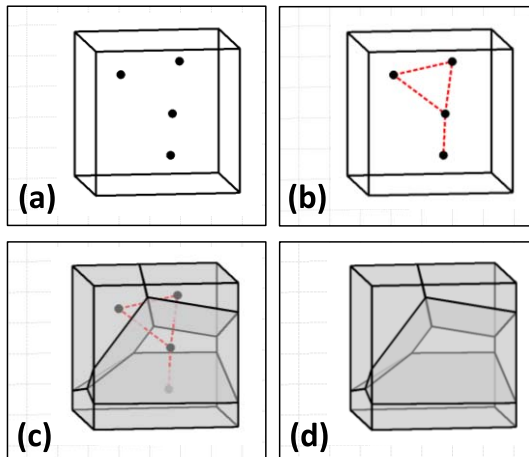


Fig. 3. Flow for constructing 3-D Voronoi patterns. (a) Randomly place grain seeds. (b) Connect every seed to its neighboring seeds (dash lines). (c) Draw perpendicular bisectors (gray planes). (d) Completed 3-D Voronoi diagram.

size, we can obtain various GB patterns by placing grain seeds randomly in a box. The number of grain seeds is determined by the following equation:

$$N = \frac{\text{box volume}}{\frac{4}{3}\pi \left(\frac{\text{grain size}}{2}\right)^3}.$$

Fig. 3 shows how the 3-D Voronoi patterns are generated. After the GB pattern is created, we capture a part of this pattern to fit in the device channel region. Finally, TCAD device simulations [16] are performed.

In our simulations, the device is designed as the junction-free BE-SONOS [6], as shown in Fig. 1. The gate-stack thicknesses for O1/N1/O2/N2/O3/G are 1.3/2/2.5/6/6/5 nm, respectively. Other pertinent parameters are listed in Table I.

A trap-concentrated GB may capture charges and form a potential barrier, which impedes free carriers [17]. Gate-induced grain barrier lowering [7] should be considered. To address the response of the current due to the lowering of energy barrier, we assume the thermionic emission transport behavior at the grain-grain interface [18]. Outside the grain-grain interface, the drift-diffusion transport is assumed. The Fermi-level pinning at GB, which has been addressed in [20] and [21], is not included in this brief.

TABLE I

DEVICE PARAMETERS USED IN THIS BRIEF

Parameter	Value
$L_g$	25 nm
$T_{ch}$	12 nm
$H_{ch}$	10 nm – 40 nm
grain size	100 nm
$O1$	1.3 nm
$N1$	2 nm
$O2$	2.5 nm
$N2$	6 nm
$O3$	6 nm
$G$	5 nm
channel doping, $N_{ch}$	n-type, $10^{16} \text{ cm}^{-3}$
gate doping, $N_G$	p-type, $10^{20} \text{ cm}^{-3}$

TABLE II

TRAP DENSITY PARAMETERS EXTRACTED FROM [18]

Parameter	Value
$g_{TD}$	$8 \times 10^{13} \text{ cm}^{-2} \text{ eV}^{-1}$
$g_{TA}$	$10^{14} \text{ cm}^{-2} \text{ eV}^{-1}$
$E_{TD}$	60 meV
$E_{TA}$	90 meV

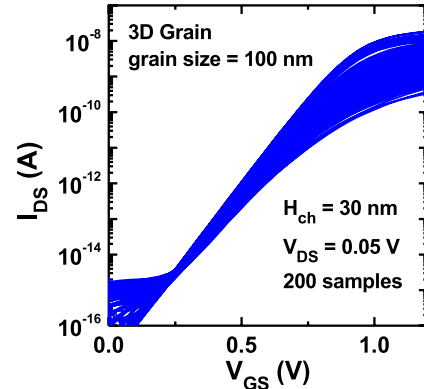


Fig. 4. Dispersion of  $I_{DS}$ - $V_{GS}$  curves due to 3-D grain patterns.

In this brief, trap states are considered as interface traps at GBs, and no other traps are assumed outside these GBs. Besides, we assume that the trap concentrations are identical for all GBs. Trap states used in this brief are obtained from fitting the experimental data [19] with the following exponential functions:

$$g_D(E) = g_{TD} \exp\left(\frac{E_V - E}{E_{TD}}\right)$$

$$g_A(E) = g_{TA} \exp\left(\frac{E - E_C}{E_{TA}}\right)$$

where  $g_D$  and  $g_A$  are donor-like and acceptor-like densities of states, respectively. The extracted parameters for  $g_{TD}$ ,  $g_{TA}$ ,  $E_{TD}$ , and  $E_{TA}$  are listed in Table II.

### III. THRESHOLD VOLTAGE VARIATION

Using our proposed 3-D Voronoi method, Fig. 4 shows the  $I_{DS}$ - $V_{GS}$  dispersion with 200 random samples. In Fig. 5, the

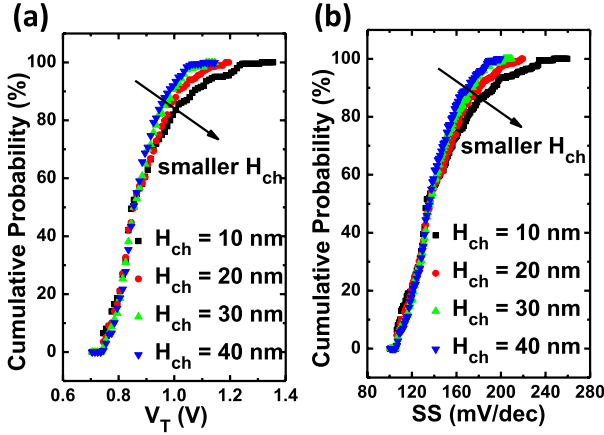


Fig. 5. Cumulative probability for (a)  $V_T$  and (b) SS for devices with various channel heights ( $H_{ch}$ ).

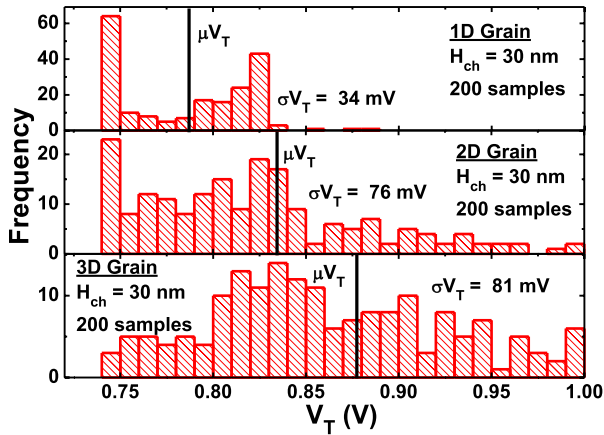


Fig. 6.  $V_T$  distributions for 1-D, 2-D, and 3-D GB patterns. The average grain size is 100 nm. Spikes are observed in both 1-D and 2-D patterns at  $V_T \approx 0.75$  V.

cumulative probabilities for  $V_T$  and subthreshold swing (SS) for devices with various channel heights ( $H_{ch}$ ) are demonstrated. It can be seen that the distributions become wider as  $H_{ch}$  shrinks, which can be explained as follows. When the device is large, there are a large amount of GBs inside the active region and their impacts on the degree of randomness are averaged by each other. In this case, the variation only comes from the different number (number fluctuation) of GBs inside each device. However, for a given average grain size, there are less GBs inside the channel as the device shrinks. Therefore, when we consider the device variability, we should no longer ignore the impact of the actual positions and shapes of these GBs. In other words, the position and shape of GBs serve as additional variation sources in addition to the number fluctuation of GBs.

The  $V_T$  distributions from 1-D rectangular, 2-D Voronoi, and 3-D Voronoi methods are compared in Fig. 6 for devices with  $H_{ch} = 30$  nm. We can observe that there is an unusual spike at  $V_T$  around 0.75 V for the 1-D and 2-D grain cases. These spikes correspond to the devices that have no GBs in their channels. On the other hand, the spike disappears for the 3-D grain case because most devices possess GBs

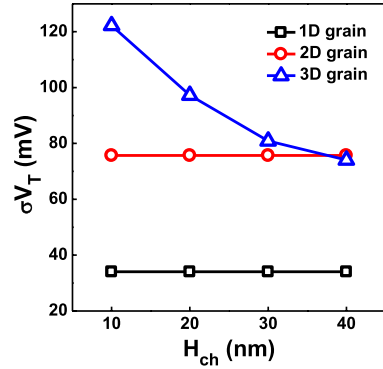


Fig. 7. Channel-height dependence of the  $V_T$  variability for 1-D, 2-D, and 3-D GB patterns.

in their channel regions and hence the devices with the smallest  $V_T$  (i.e., no GB) become rare. Fig. 7 compares the  $H_{ch}$  dependence of  $V_T$  variations for the 1-D, 2-D, and 3-D methods. It can be seen that the 1-D and 2-D methods tend to underestimate the  $\sigma V_T$  for devices with scaled  $H_{ch}$ . Compared with the 1-D and 2-D grains, the 3-D grain has more freedom in varying the GB shapes, thus exhibiting a larger  $V_T$  variability. It indicates that a full 3-D GB pattern needs to be employed to accurately simulate the GB-induced variability.

#### IV. CONCLUSION

We have investigated the random GBs-induced variability in poly-Si thin-film transistor using 3-D Voronoi grain patterns. Compared with the 1-D and 2-D methods, the 3-D Voronoi grain can show a more realistic variability when devices are downscaled along the channel height ( $H_{ch}$ ) direction. This brief indicates that a full 3-D consideration is needed when modeling the random GB-induced threshold-voltage variation.

#### ACKNOWLEDGMENT

The authors would like to thank the National Center for High-Performance Computing in Taiwan for the computational software and facilities.

#### REFERENCES

- [1] H. Tanaka *et al.*, "Bit cost scalable technology with punch and plug process for ultra high density flash memory," in *VLSI Symp. Tech. Dig.*, 2007, pp. 14–15.
- [2] R. Katsumata *et al.*, "Pipe-shaped BiCS flash memory with 16 stacked layers and multi-level-cell operation for ultra high density storage devices," in *VLSI Symp. Tech. Dig.*, 2009, pp. 136–137.
- [3] J. Jang *et al.*, "Vertical cell array using TCAT (terabit cell array transistor) technology for ultra high density NAND flash memory," in *VLSI Symp. Tech. Dig.*, 2009, pp. 192–193.
- [4] J. Kim *et al.*, "Novel vertical-stacked-array-transistor (VSAT) for ultra-high-density and cost-effective NAND flash memory devices and SSD (solid state drive)," in *VLSI Symp. Tech. Dig.*, 2009, pp. 186–187.
- [5] W. Kim *et al.*, "Multi-layered vertical gate NAND flash overcoming stacking limit for terabit density storage," in *VLSI Symp. Tech. Dig.*, 2009, pp. 188–189.
- [6] H.-T. Lue *et al.*, "A highly scalable 8-layer 3D vertical-gate (VG) TFT NAND flash using junction-free buried channel BE-SONOS device," in *VLSI Symp. Tech. Dig.*, 2010, pp. 131–132.

- [7] Y.-H. Hsiao *et al.*, "Modeling the variability caused by random grain boundary and trap-location induced asymmetrical read behavior for a tight-pitch vertical gate 3D NAND flash memory using double-gate thin-film transistor (TFT) device," in *IEDM Tech. Dig.*, 2012, pp. 609–612.
- [8] E. Nowak *et al.*, "Intrinsic fluctuations in vertical NAND flash memories," in *VLSI Symp. Tech. Dig.*, 2012, pp. 21–22.
- [9] O. K. B. Lui, M. J. Quinn, S. W.-B. Tam, T. M. Brown, P. Migliorato, and H. Ohshima, "Investigation of the low field leakage current mechanism in polysilicon TFT's," *IEEE Trans. Electron Devices*, vol. 45, no. 1, pp. 213–217, Jan. 1998.
- [10] C.-H. Ho, G. Panagopoulos, and K. Roy, "A physical model for grain-boundary-induced threshold voltage variation in polysilicon thin-film transistors," *IEEE Trans. Electron Devices*, vol. 59, no. 9, pp. 2396–2402, Sep. 2012.
- [11] T.-K. A. Chou and J. Kanicki, "Two-dimensional numerical simulation of solid-phase-crystallized polysilicon thin-film transistor characteristics," *Jpn. J. Appl. Phys.*, vol. 38, no. 4B, pp. 2251–2255, Apr. 1999.
- [12] Y. Kitahara, S. Takagi, and N. Sano, "Statistical study of subthreshold characteristics in polycrystalline silicon thin-film transistors," *J. Appl. Phys.*, vol. 94, no. 12, pp. 7789–7795, Nov. 2003.
- [13] C.-W. Yang and P. Su, "Simulation of grain-boundary induced  $V_{th}$  variability in stackable NAND flash using a Voronoi approach," in *Proc. NVMTS*, Nov. 2012, pp. 93–94.
- [14] S.-H. Chou, M.-L. Fan, and P. Su, "Investigation and comparison of work function variation for FinFET and UTB SOI devices using voronoi approach," *IEEE Trans. Electron Devices*, vol. 60, no. 4, pp. 1485–1489, Apr. 2013.
- [15] A. Okabe, B. Boots, and K. Sugihara, *Spatial Tessellations Concepts and Applications of Voronoi Diagrams*. New York, NY, USA: Wiley, 1992.
- [16] *Sentaurus TCAD, G2012-06 Manual*, Synopsys, Inc., Mountain View, CA, USA, 2012.
- [17] J. G. Fossum and A. Ortiz-Conde, "Effects of grain boundaries on the channel conductance of SOI MOSFET's," *IEEE Trans. Electron Devices*, vol. 30, no. 8, pp. 933–940, Aug. 1983.
- [18] J. Y. W. Seto, "The electrical properties of polycrystalline silicon films," *J. Appl. Phys.*, vol. 46, no. 12, pp. 5247–5254, Dec. 1975.
- [19] M. Kimura *et al.*, "Extraction of trap states in laser-crystallized polycrystalline-silicon thin-film transistors and analysis of degradation by self-heating," *J. Appl. Phys.*, vol. 91, no. 6, pp. 3855–3858, Mar. 2002.
- [20] A. Brown, G. Roy, and A. Asenov, "Poly-Si-gate-related variability in decanano-meter MOSFETs with conventional architecture," *IEEE Trans. Electron Devices*, vol. 54, no. 11, pp. 3056–3063, Nov. 2007.
- [21] A. Brown, G. Roy, and A. Asenov, "Impact of Fermi level pinning at polysilicon gate grain boundaries on nano-MOSFET variability: A 3-D simulation study," in *Proc. 36th ESSDERC*, 2006, pp. 451–454.
- [22] G. Roy, A. Ghetti, A. Benvenuti, A. Erlebach, and A. Asenov, "Comparative simulation study of the different sources of statistical variability in contemporary floating gate non-volatile memory," *IEEE Trans. Electron Devices*, vol. 58, no. 12, pp. 4155–4163, Dec. 2011.



**Ching-Wei Yang** received the B.S. degree from the Electrical Engineering and Computer Science Undergraduate Honors Program, National Chiao Tung University, Hsinchu, Taiwan, and the M.S. degree from the Department of Electronic Engineering, National Chiao Tung University, in 2011 and 2013, respectively.



**Pin Su** (S'98–M'02) received the Ph.D. degree from the University of California at Berkeley, Berkeley, CA, USA.

He is currently a Professor with the Department of Electronics Engineering, National Chiao Tung University, Hsinchu, Taiwan.

Prof. Su served in the Technical Committee of the International Electron Devices Meeting from 2012 to 2013.